ADVANCED FUNCTIONAL MATERIALS

www.afm-journal.de

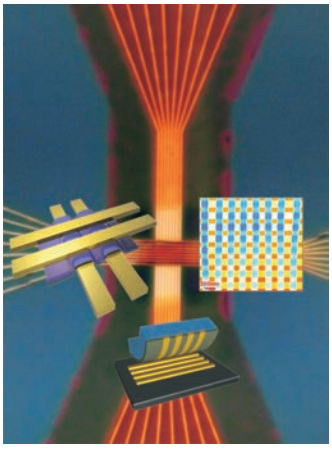

Surface Patterning

On page 1129, Dirk Mayer and co-workers report the non-invasive assembly of highly integrated metal-bridge-metal crossbar junctions under ambient conditions by combining nanoimprint lithography and soft lithography. Different views of the printing process and ready assembled crossbar arrays are shown. Conductive polymer films are incorporated in the cross points to evaluate the utility and versatility of the soft lithography approach.

Organic Spintronics

Spin-polarized transport in organic spin valves remains poorly understood, despite their promising properties. On page 1180, Michel P. de Jong and co-workers report a joint experimental and modeling study on C_{60}-based spin valves that constitutes a significant step forward. For spin-polarized tunneling via multiple intermediate states in the C_{60} layer, the magnetoresistance decreases with the number of tunnel steps regardless of the value of the spin lifetime, which is analogous to conductivity mismatch in diffusive semiconductor systems.

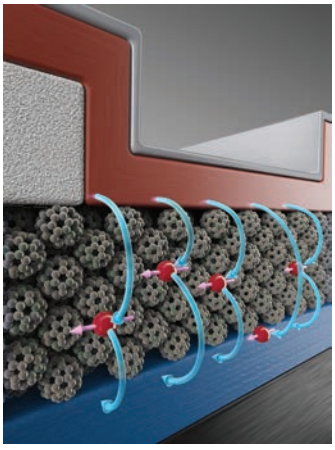

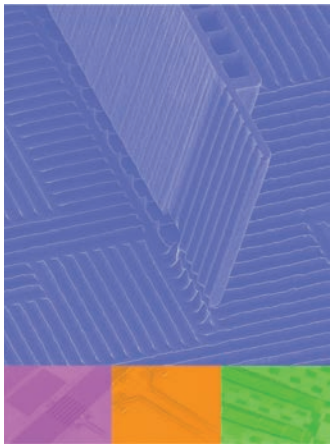

Silicon Micromachining

On page 1222, Giuseppe Barillaro and co-workers demonstrate that electrochemical micromachining (ECM) technology allows the fabrication of silicon microstructures with various shapes and silicon microsystems with high complexity to be performed in any research laboratory with sub-micrometer accuracy up to the highest aspect ratio values using dynamical real-time control of the etching anisotropy. False-color scanning electron microscopy (SEM) images of a silicon microgripper fabricated using ECM technology are acquired at different magnifications.

CONTENTS

CORRESPONDENCE

FEATURE ARTICLE

Solar Cells

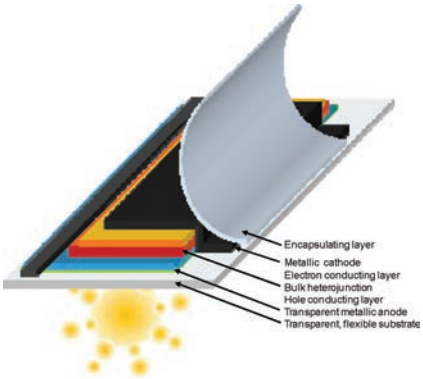

Recent experiments that investigate the recombination loss processes in organic bulk heterojunction solar cells, ranging from photoexcitation to charge transfer, recombination, and collection, are described. The study of recombination loss processes in optimized and intentionally unoptimized systems leads to insights into what must be accomplished to achieve the "ideal" solar cell.

FULL PAPER

Surface Patterning

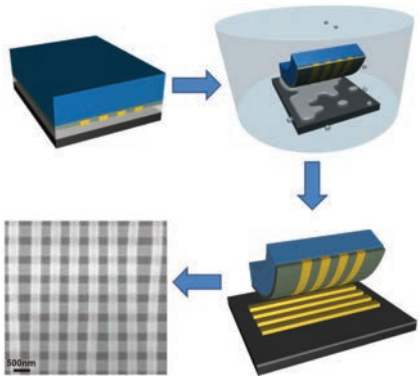

Metal electrode crossbar arrays with feature sizes in the nanometer range are fabricated by combining nanoimprint lithography with a universal and gentle printing method. The feasibility of this process is demonstrated by assembling 8 bit × 8 bit crossbar arrays. Metal–molecule metal junctions are realized and electrically characterized by incorporating two types of conductive polymers into the crossbar structures.

FULL PAPERS

A new process for the preparation of functionalized graphene dispersions without surfactants or additives is described. This simple process is suitable for large-scale production and a wide range of concentrations including highly viscous graphene pastes. These pastes can be used in a printing process based on 3D microextrusion to form electrically conducting patterns and coatings.

Flexible Electronics

Arrhenius plots of lithium fluoride thin films grown on silica substrates during various heating–stabilization–cooling cycles allow three Li^+-migration paths in the inner film, with different local conductivities, to be distinguished. A remarkable enhancement of the Li-ion conductivity arises from the formation of a significant density of glass/ceramic interfaces, enabling percolation of interfacial or amorphous pathways.

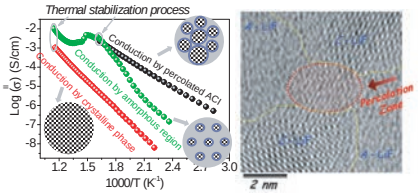

Interfaces

A 10-fold rotational symmetric quasicrystal pattern can be fabricated by multiple exposure interference lithography. The photonic band gap of the structure is calculated via finite difference time domain. The impacts of the rotational symmetry, filling ratio, and phase parameter on the photonic band gap are discussed.

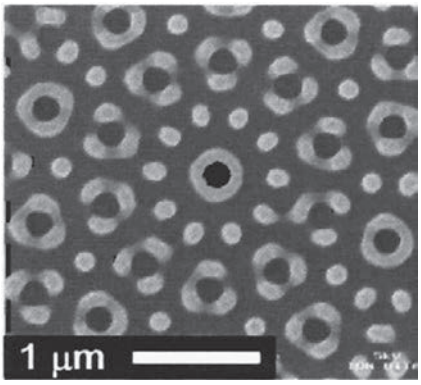

Photonics

Porous silicon (pSi) surfaces are patterned with dual alkene compounds by means of a UV-initiated hydrosilylation reaction through a photomask. Patterned surface attachment of an *N*-hydroxysuccinimide (NHS) ester functionalized alkene with a polyethylene glycol (PEG) alkene attached in the surrounding areas allows patterned conjugation of the cell adhesion mediator protein fibronectin to pSi surfaces. Protein functionalized surfaces are successfully used for the guided attachment of mammalian neuronal cells.

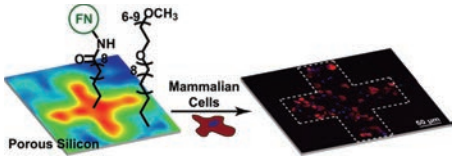

Biomedical Applications

CONTENTS

FULL PAPERS

Photovoltaics

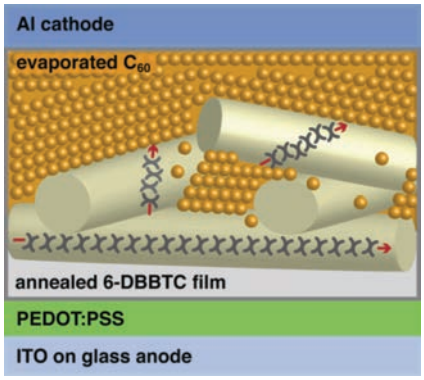

Self assembly can be exploited to engineer the interface and morphology between the single crystal cables of donor material (6-DBTTC) and polycrystalline acceptor (C_{60}) to create an interpenetrating network of pure phases expected to be optimal for photovoltaic device performance. These strategies facilitate 3D nanostructured photovoltaic cells made with the simplicity and control of bilayer device fabrication.

Nanoparticles

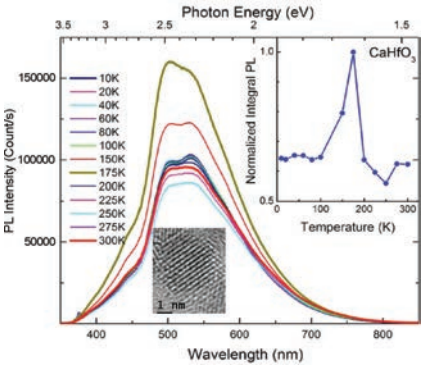

Optical properties of $SrHfO_3$ and $CaHfO_3$ nanoparticles with sizes as small as 1.6 nm are reported. An unexpected and strong luminescence from the undoped nanoparticles is observed in the visible spectrum over a wide temperature range, also exhibiting sensitivity to temperature variation and surrounding ambient (vacuum/air) as well as exposure time to UV light.

Spintronics

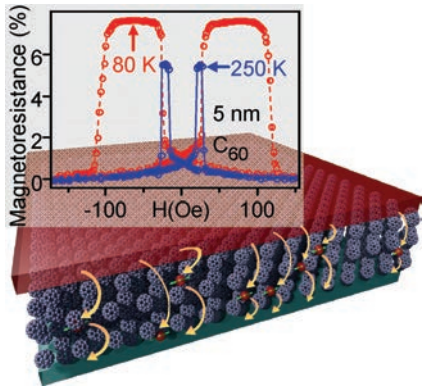

Organic spin valves show many promising features but remain poorly understood. An experimental study of C_{60}-based spin valves is presented and their behavior is modeled with spin-polarized tunneling via multiple intermediate states. Analogous to the conductivity mismatch in the diffusive regime, the magnetoresistance decreases with the number of intermediate tunnel steps, regardless of the value of the spin lifetime.

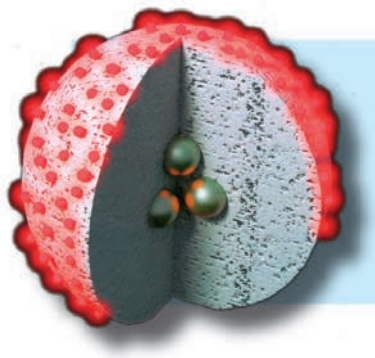

How to contact us:

Editorial Office:
Phone: (+49) 6201-606-235/531
Fax: (+49) 6201-606-500
Email: afm@wiley-vch.de

Reprints:
cherth@wiley-vch.de

Copyright Permission:
Fax: (+49) 6201-606-332
Email: rights@wiley-vch.de

FULL PAPERS

For crystalline silicon nanoparticles (Si-ncs), various low-cost post-growth treatments are presented that efficiently reduce the number of charge-trapping defects in the Si-ncs and remove the native oxide that forms upon exposure to air and hinders the charge transport. Particularly promising are HF-etched plus vacuum-annealed Si-ncs leading to a strong conductivity enhancement in thin films and HF-etched plus hydrosilylated Si-ncs that are extremely stable against reoxidation.

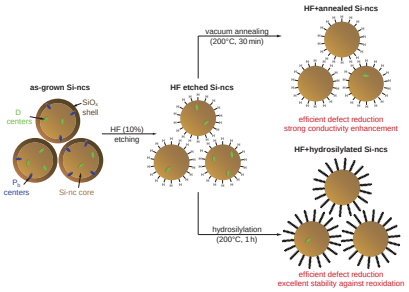

Nanoparticles

Low-Cost Post-Growth Treatments of Crystalline Silicon Nanoparticles Improving Surface and Electronic Properties

Recombinant human gelatin conjugated with lipoic acid (rHG-LA) forms nanoparticles spontaneously in aqueous solution and encapsulates alpha-tocopheryl succinate (α-TOS), a well-known cancer-selective apoptosis-inducing agent. The promising applicability of α-TOS-loaded rHG-LA nanoparticles with passive targeting ability and cancer cell-specific apoptosis is described.

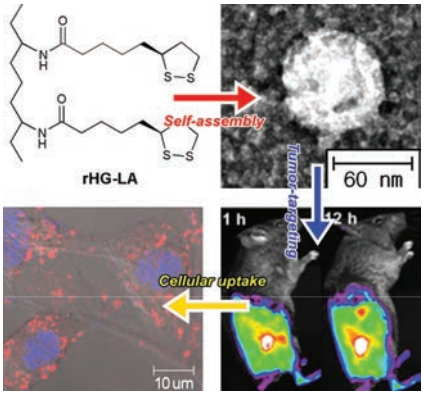

Drug Delivery

Self-Assembled Nanoparticles with Dual Effects of Passive Tumor Targeting and Cancer-Selective Anticancer Effects

A self-aligned multi-level embossing patterning method for manufacturing bottom-gate, bottom-contact thin-film transistors on flexible substrates is demonstrated. The low temperature processed metal-insulator-metal stack includes an optimized defect-free, flat, and uniform gate dielectric layer based on aluminum anodization. Electrical measurements exhibit promising transfer characteristics of the devices, proving the feasibility of this technique.

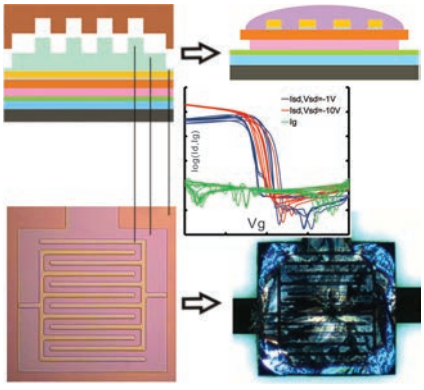

Transistors

Organic Thin-Film Transistors with Anodized Gate Dielectric Patterned by Self-Aligned Embossing on Flexible Substrates

Robust hollow spheres consisting of molecular-scale alternating titania ($Ti_{0.91}O_2$) nanosheets and graphene (G) nanosheets are successfully fabricated using a layer-by-layer assembly technique. The nanostructures exhibit high efficiency of photocatalytic conversion of CO_2 into renewable fuels.

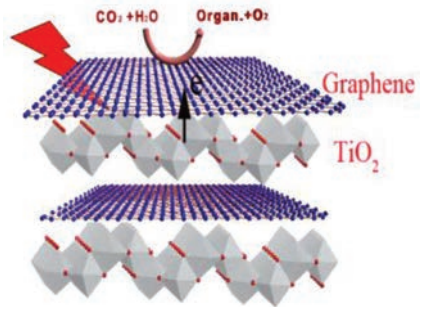

Catalysis

Robust Hollow Spheres Consisting of Alternating Titania Nanosheets and Graphene Nanosheets with High Photocatalytic Activity for CO_2 Conversion into Renewable Fuels

CONTENTS

FULL PAPERS

Microstructures

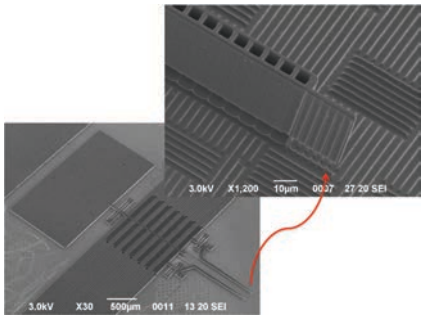

The advanced fabrication of silicon microstructures of various shapes and silicon microsystems of high complexity using electrochemical micromachining (ECM) technology is described. ECM technology makes use of a dynamic control of the electrochemical etching anisotropy, which allows silicon dissolution to be switched in real-time from the anisotropic to the isotropic regime, to enable the low-cost fabrication of microstructures and microsystems using both functional and sacrificial structures.

Self-Assembly

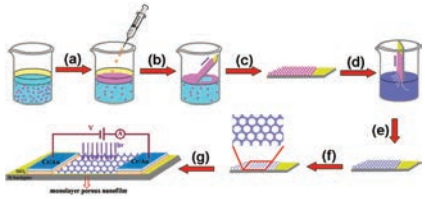

2D ordered SnO_2 monolayer nanofilm and other semiconducting metal-oxide nanofilms such as TiO_2, ZnO, and CeO_2 can be easily fabricated using polymer monolayer nanofilms prepared by oil–water interfacial self-assembly as sacrificial templates. The first 2D ordered SnO_2 monolayer nanofilm-based UV photodetector is successfully constructed. This photodetector exhibits ultrahigh photocurrent and sensitivity, excellent stability, and reproducible characteristics.

Solar Cells

A new multiscale stochastic model accurately describes and models the morphology of disordered polymer–zinc oxide solar cells as a function of processing parameters in terms of structural and physical blend characteristics including domain connectivity, charge carrier mobility, and exciton quenching efficiency. A key result is that increasing the spin-coating velocity leads to coarse morphology.

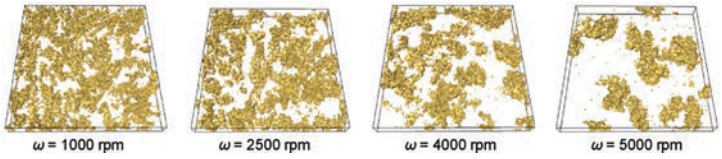

Bioinspired Materials

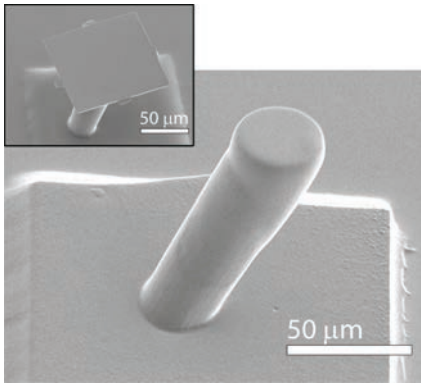

Gecko-inspired angled elastomer micropillars with flat or round tip endings are presented as compliant pick-and-place micromanipulators. The pillars are 35 µm in diameter, 90 µm tall, and angled at an inclination of 20°. Through shear displacement control, pick-to-release attachment force ratios of 39 to 1 are achieved and micromanipulation is demonstrated.

FULL PAPERS

^{1}H spin diffusion NMR is demonstrated to be a valuable method for estimating the domain sizes in polymer:fullerene (poly-3-hexylthiophene:phenyl-C61-butyric acid methyl ester (P3HT:PCBM)) thin-film blends for bulk heterojunction photovoltaic devices. Variations in spin-casting speed and thermal annealing schedule have dramatic effects on the domain sizes observed in the blend films, which in turn affects the power conversion efficiency.

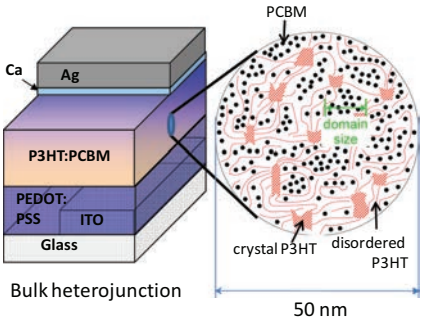

Photovoltaic Devices

1D Cu-nanowire-doped graphene (Cu NWs/graphene) is used as the back contact for CdTe solar cells. The efficiency of cells with the Cu NWs/graphene reaches up to 12.1%, which is higher than for those with traditional back contacts using Cu-particle-doped graphite (10.5%) or Cu thin films (9.1%). The Cu-NW cells also exhibit an excellent thermal stability.

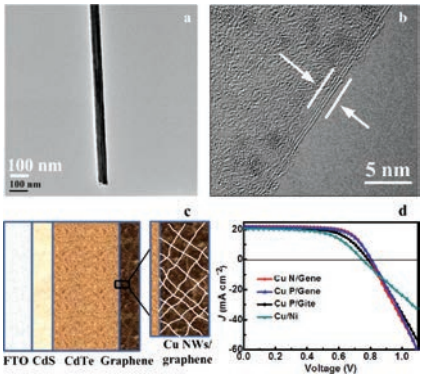

Solar Cells

A high energy density asymmetric supercapacitor is developed based on an additive-free, nano-architectured $Ni(OH)_2$/CNT electrode with an ultra-high specific capacitance of 3300 F g^{-1} and high areal capacitance of 16 F cm^{-2}. This asymmetric supercapacitor prototype is able to power up a 3 V mini-fan for 90 s by 10 s charging with an AA battery.

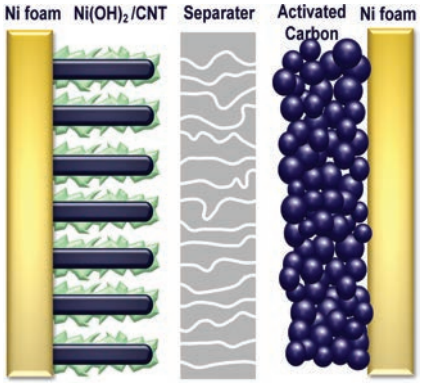

Electrodes

Wavy carbon nanotube ribbons coated with a thin layer of metal film are fabricated on poly(dimethylsiloxane) (PDMS) substrates through mechanical buckling. Covered with a top layer of PDMS, the wavy nanotube ribbons are able to accommodate large stretching (up to 100%) with little change in resistance. The resistance stabilizes upon further unloading and reloading.

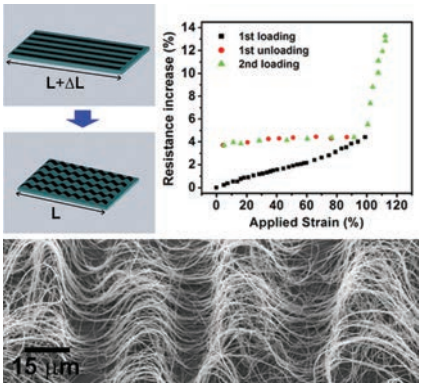

Carbon Nanotubes

FULL PAPERS

Supercapacitors

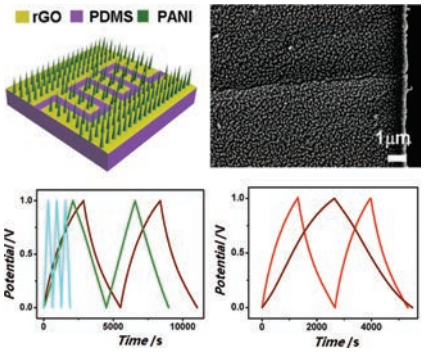

Microelectrodes of an all-solid-state flexible micro-supercapacitor are prepared using in situ electrodeposition of polyaniline nanorods onto the surface of reduced graphene oxide patterns. The micro-supercapacitor possesses high electrochemical capacitance and good stability.

Structure–Property Relationships

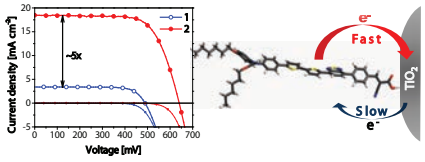

Two donor-π-acceptor dyes are synthesized for application in dye-sensitized solar cells (DSSCs). The introduction of a phenyl ring between benzothiadiazole and cyanoacrylic acid acceptors leads to an over six times higher efficiency in DSSCs compared to the sensitizer without phenyl unit due to inhibition of back electron transfer and a reduced recombination rate.

Solar Cells

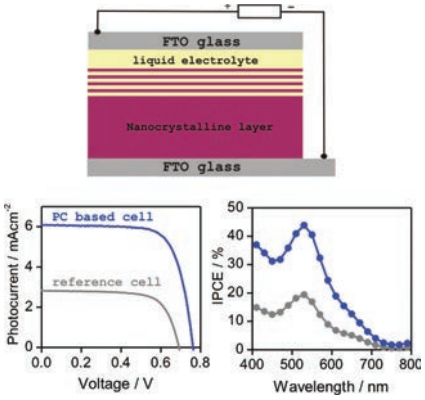

Highly efficient, thin, dye-sensitized solar cells can be designed through the integration of 1D photonic structures of optimized porosity, with increases in both the device photocurrent and the photovoltage. Devices with enhanced efficiency are obtained while preserving the transparency, which is a topic of major interest due to possible applications in building integrated photovoltaics (BIPV).

Composite Materials

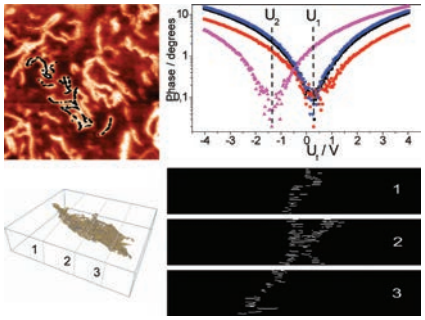

The conductive graphene network in a conductive graphene/polystyrene composite sample is separated from electrically isolated graphene sheets by analyzing the same area with conductive atomic force microscopy (C-AFM) and electrostatic force microscopy (EFM). The novel technique based on combination of a scanning probe microscope and microtome is utilized for 3D reconstruction of the graphene sheets in the polymer matrix with *z*-resolution in the order of ≈ 10 nm.